Molecular Biology of the Cell
Vol. 19, 4076–4085, October 2008

Interaction between Tumor Suppressor Adenomatous Polyposis Coli and Topoisomerase IIα: Implication for the G2/M Transition

Yang Wang,* Yoshiaki Azuma,* David Moore,† Neil Osheroff,‡ and Kristi L. Neufeld*

*Department of Molecular Biosciences and †KU Microscopy and Analytical Imaging Laboratory, University of Kansas, Lawrence, KS 66045; and ‡Department of Biochemistry, Vanderbilt University School of Medicine, Nashville, TN 37232

Submitted January 2, 2008; Revised June 3, 2008; Accepted July 8, 2008
Monitoring Editor: Yixian Zheng

The tumor suppressor adenomatous polyposis coli (APC) is implicated in regulating multiple stages of the cell cycle. APC participation in G1/S is attributed to its recognized role in Wnt signaling. APC function in the G2/M transition is less well established. To identify novel protein partners of APC that regulate the G2/M transition, APC was immunoprecipitated from colon cell lysates and associated proteins were analyzed by matrix-assisted laser desorption ionization/time of flight (MALDI-TOF). Topoisomerase IIα (topo IIα) was identified as a potential binding partner of APC. Topo IIα is a critical regulator of G2/M transition. Evidence supporting an interaction between endogenous APC and topo IIα was obtained by coimmunoprecipitation, colocalization, and Förster resonance energy transfer (FRET). The 15-amino acid repeat region of APC (M2-APC) interacted with topo IIα when expressed as a green fluorescent protein (GFP)-fusion protein in vivo. Although lacking defined nuclear localization signals (NLS) M2-APC predominantly localized to the nucleus. Furthermore, cells expressing M2-APC displayed condensed or fragmented nuclei, and they were arrested in the G2 phase of the cell cycle. Although M2-APC contains a β-catenin binding domain, biochemical studies failed to implicate β-catenin in the observed phenotype. Finally, purified recombinant M2-APC enhanced topo IIα activity in vitro. Together, these data support a novel role for APC in the G2/M transition, potentially through association with topo IIα.

INTRODUCTION

The tumor suppressor protein adenomatous polyposis coli (APC) is inactivated in >80% of all colorectal cancers (Kinzler and Vogelstein, 1996). The detection of mutant APC in the earliest stages of polyp development supports the idea that mutation of *APC* is an initiating event in colon carcinogenesis. The most common form of *APC* mutation results in elimination of the carboxy-terminal half of the APC protein. Because APC is a large, multidomain protein, APC truncation is predicted to impact several cellular mechanisms, the extent of which we are only beginning to understand.

There is accumulating evidence supporting a role for APC in the regulation of cell cycle. Overexpression of APC in NIH3T3 fibroblasts and colon cancer cell lines leads to G1 cell cycle arrest (Ishidate *et al*., 2000; Heinen *et al*., 2002), presumably by repressing transcription of Wnt targets such as cyclin D1. APC may also participate directly in mitosis because it is transiently hyperphosphorylated in the M phase of the cell cycle (Bhattacharjee *et al*., 1996), accumulates at the microtubule-organizing center (Olmeda *et al*., 2003), and associates with the kinetochore in dividing cells (Fodde *et al*., 2001; Kaplan *et al*., 2001). A role for APC in mitosis might be critical for regulation of genomic stability and proper chromosome segregation. APC stabilized by zinc treatment induces G2/M cell cycle arrest in colon cancer cells (Jaiswal and Narayan, 2004). However, to date, little is known about the underlying mechanism by which APC participates in the G2/M cell cycle transition.

Here, we report identification of topoisomerase IIα (topo IIα) as a potential APC-binding protein. Topo IIα enzyme catalyzes DNA topology changes by introducing double-strand DNA breaks that facilitate DNA strand passage and subsequent DNA religation (Wang, 1996; Champoux, 2001; Fortune and Osheroff, 2001; McClendon and Osheroff, 2007). Topo IIα has been implicated in several cellular functions such as DNA replication and chromosome condensation (Wang, 1996; Nitiss, 1998; Fortune and Osheroff, 2000; Champoux, 2001; Wang, 2002; McClendon and Osheroff, 2007), and it seems to be essential in the control of the G2/M decatenation checkpoint during cell division (Downes *et al*., 1994). Topo IIα was also found to be deregulated in colon cancers, with its expression limited to the proliferative zone in the normal colon, but up-regulated and widespread in colon cancer tissue (Murphy *et al*., 2001). At primary locations of recurrent malignant colon tumors after chemotherapy, the number of topo IIα-positive cells is greatly increased compared with primary sites with no recurrence (Lazaris *et al*., 2002), suggesting that changes in topo IIα expression occur subsequent to *APC* mutation. Together,

This article was published online ahead of print in *MBC in Press* (http://www.molbiolcell.org/cgi/doi/10.1091/mbc.E07–12–1296) on July 16, 2008.

Address correspondence to: Kristi L. Neufeld (klneuf@ku.edu).

Abbreviations used: APC, adenomatous polyposis coli; FRET, Förster resonance energy transfer; NLS, nuclear localization signal; topo IIα, topoisomerase IIα; FACS, fluorescence activated cell sorting; GFP, green fluorescent protein.

these observations make topo IIα an attractive candidate for mediating the G2/M cell cycle transition.

Overexpression of an APC fragment that interacts with topo IIα in various colon cancer cells lines led to abnormal nuclear morphology and cell cycle inhibition in G2. Our data suggest a novel role for nuclear APC in the regulation of cell cycle progression, potentially through an interaction with topo IIα.

MATERIALS AND METHODS

Cell Culture and DNA Constructs

HCT116βw cells (a generous gift from Dr. Bert Vogelstein) were grown in McCoy's 5A medium (Invitrogen) supplemented with 10% fetal bovine serum (FBS) (HyClone Laboratories, Logan, UT). Expression constructs for APC fragments fused to green fluorescent protein (GFP) were kindly provided by Dr. Kozo Kaibuchi and have been described previously (Watanabe *et al*., 2004).

Antibodies and Immunofluorescence Microscopy

Immunostaining was performed as described previously (Neufeld and White, 1997) and the following antibodies were used: anti-APC (ab-7, 1:50; Calbiochem, San Diego, CA), anti-APC (ab-4, 1:2000; Calbiochem), anti-APC (ab-1, 1:100; Calbiochem), anti-topo IIα (1:100; Research Diagnostics, Flanders, NJ), anti-phospho-histone H3 (1:500; Millipore, Billerica, MA), anti-β-catenin (1:200; BD Biosciences Transduction Laboratories, Lexington, KY), and anti-proliferating cell nuclear antigen (PCNA, 1:1000; BD Biosciences Transduction Laboratories); goat anti-mouse immunoglobulin G (IgG) Alexa 488 (1:1000; Invitrogen, Carlsbad, CA), goat anti-rabbit IgG Alexa 568 (1:1000; Invitrogen), and goat anti-mouse IgG Alexa 610-R-phycoerythrin (1:500; Invitrogen). DNA was labeled with Topro-3 (1:500; Invitrogen), or 4,6-diamidino-2-phenylindole (DAPI) (1:5000; Invitrogen). Two-dimensional (2-D) and three-dimensional (3-D) distributions of immunofluorescent signals were examined using a Yokugawa-type spinning disk confocal microscope equipped with an Olympus 150× objective with a numerical aperture of 1.45 and 1KX1K EMCCD (Olympus and Intelligent Imaging Innovations, Denver, Co.). From >200 cells that were viewed, 50 cells were randomly chosen to be imaged. At least 24 image frames were collected at z-intervals of 100 nm for image sets where 3-D colocalization was examined. No deconvolution was performed. All raw confocal image series were analyzed by ImageJ program (National Institutes of Health, Bethesda, MD) and the JACoP plugin without further processing. Mitotic indices were determined by counting DAPI-stained mitotic cells in a field of 100 cells for each repetition.

Protein Colocalization Analysis

Colocalization coefficients were calculated using ImageJ and the JACoP plugin (Bolte and Cordelieres, 2006). Using Costes' method of automatic threshholding, a Pearson's coefficient was calculated for pixels within all of the calculated regions of interest in an image where Alexa 488 and Alexa 568 fluorescence were each detected at levels significantly above background. Mander's coefficients were also calculated to determine the degree of overlap between the corresponding regions of detected signals.

Förster Resonance Energy Transfer (FRET) Analysis

Evidence of FRET between secondary fluorophores was detected using a Zeiss 510 Meta spectral imaging upright laser scanning confocal microscope (Carl Zeiss, Thornwood, NY). Donor fluorescence, alternatively from Alexa 488 or Alexa 610-R-phycoerythrin was photobleached by passing the beam of the 543-nm laser (at 100% output) over defined regions of interest for 75 iterations or by using 200 passes of the 633-nm laser (also 100% output). Proximity of the two proteins was determined by calculating the mean FRET efficiency between donor and acceptor according to the method of Kenworthy and Edidin (1998), where $E = 100(\text{Alexa } 488_{post} - \text{Alexa } 488_{pre})/\text{Alexa } 488_{post}$ or $E = 100(\text{Alexa 610-R-PE}_{post} - \text{Alexa 610-R-PE}_{pre})/\text{Alexa 610-R-PE}_{post}$. All pixels within the photobleached regions were used for these calculations. Error bars indicate the SEM. Three-dimensional reconstructions and projections were also performed with ImageJ.

Immunoprecipitation and Western Immunoblots

Immunoprecipitation (IP) and Western immunoblots (IB) were performed using modified standard protocols. Cells at 90% confluence were lysed in lysis buffer (50 mM Tris, pH 7.5, 0.1% NP-40, 100 mM NaCl, 1 mM $MgCl_2$, 5 mM EDTA, protease inhibitor cocktail [Sigma-Aldrich, St. Louis, MO], and Halt phosphatase inhibitor cocktail [Pierce Chemical, Rockford, IL]) on ice for 30 min. Cell lysates were sonicated for 10 pulses, level 1 with 10% output, three times. Specific antibodies were preincubated with protein A Dynabeads (Invitrogen) for 2 h at room temperature. Dynabeads saturated with antibodies were added to 1 mg of soluble lysate and incubated overnight at 4°C. IP pellets were subject to two washes of 15 min by using lysis buffer and one wash using phosphate-buffered saline (PBS)/Tween 20 at 4°C. The following antibodies were used for IP: anti-topo IIα sera (a generous gift from Dr. Joe Holden), affinity-purified anti-APC-M2 rabbit polyclonal antibody made against amino acids 1000–1326, and polyclonal anti-GFP (Invitrogen). Immunoblots were probed with the following antibodies: anti-APC (ab-1, 1:100; Calbiochem), anti-APC-M2 polyclonal (1:4000), anti-β-catenin (1:2000; Sigma-Aldrich), anti-topo IIα (1:1000; Research Diagnostics), anti-topo IIβ (1:1000; Santa Cruz Biotechnology, Santa Cruz, CA), and anti-α-tubulin (1:2000; Calbiochem).

Transfection and Reporter Gene Assay

HCT116βw, SW480, and HCA7 cells were transfected using Lipofectamine 2000 reagent according to the manufacturer's protocol (Invitrogen). For luciferase assays, HCT116βw cells grown in 24-well plates were cotransfected with 2 μg of the GFP-M2-APC or GFP expression construct, 100 ng of the TCF-reporter construct SuperTOP-flash or FOPflash (Millipore), and 50 ng of the pRL-TK *Renilla* luciferase construct (Promega, Madison, WI) as a control to normalize the transfection efficiency. After 24 h, cells were harvested and luciferase activities were determined using Dual-Luciferase assay system (Promega) and a TD-20/20 luminometer (Turner Designs, Sunnyvale, CA). SuperTOP-flash and FOPflash luciferase activities were first normalized by pRL-TK *Renilla* luciferase, and then the normalized SuperTOP-flash luciferase activity was divided by normalized FOPflash luciferase activity to calculate relative β-catenin activity.

Fluorescence Activated Cell Sorting (FACS) Analysis

Propidium iodide staining of GFP-expressing cells in suspension was performed using a standard protocol as described previously (Lamm *et al*., 1997). HCT116βw cells at 35% confluence were transfected using Lipofectamine 2000 (Invitrogen). Thirty hours after transfection, cells were fixed with 2% paraformaldehyde (Electron Microscopy Sciences, Hatfield, PA) on ice for 1 h, followed by overnight permeabilization by using 70% ethanol in PBS. Rehydrated cells were then stained with 40 μg/ml propidium iodide (Sigma-Aldrich) in PBS for 30 min at 37°C. FACS analysis was performed using an FACScan (BD Biosciences, San Jose, CA).

Topo IIα Assays and Recombinant Proteins

To generate recombinant S tag fused M2-APC, the corresponding cDNA for APC (amino acids 1000–1326) was subcloned into a pET-30a(+) vector. Both tags (S and His) were fused to the amino terminus of the protein. The expression and purification of S-M2-APC fusion protein was performed as described previously (Azuma *et al*., 2003). Recombinant human topo IIα was made as described previously (Worland and Wang, 1989; Kingma *et al*., 1997). In vitro topo IIα relaxation and decatenation assays were performed as described previously (Fortune and Osheroff, 2001).

RESULTS

Endogenous Full-Length APC Associates with Topo IIα

To identify novel APC-binding proteins that could potentially function to regulate cell cycle progression, we immunoprecipitated APC from HCT116 cell lysates, resolved precipitated proteins by SDS-polyacrylamide gel electrophoresis, and visualized these proteins using Coomassie Blue stain. One protein in a 170-kDa band unique to the APC precipitation was identified by MALDI-TOF analysis as topo IIα (Neufeld and White, unpublished data).

We verified the APC–topo IIα interaction in both HCT116 cells and cells derived from this cell line. Although HCT116 cells were initially cultured from human colon cancer tissue, they express full-length APC and maintain a stable karyotype. The original HCT116 cell line possesses one wild-type and one mutant β-catenin allele. The mutant allele encodes a stabilized version of β-catenin, which is not down-regulated by APC. The HCT116βw line we use for most experiments was engineered to eliminate the mutant β-catenin allele; thus, it expresses only wild-type β-catenin protein (Chan *et al*., 2002). Full-length endogenous APC coimmunoprecipitated with topo IIα in HCT116 cell lysates (Figure 1A). No full-length APC was precipitated with control rabbit IgG. In reciprocal experiments, topo IIα coprecipitated with full-length APC by using an affinity-purified APC antibody, but not with preimmune sera (Figure 1B, left). We consis-

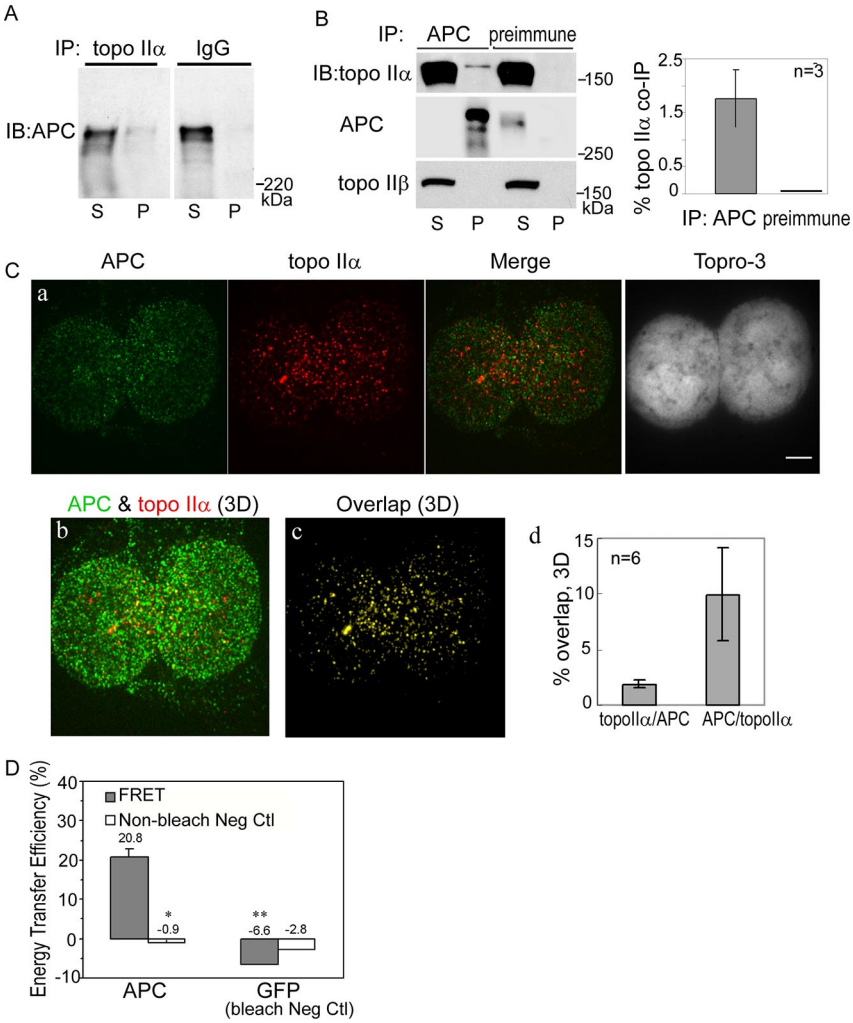

Figure 1. Endogenous topo IIα associates with endogenous full-length APC. (A) Endogenous full-length APC coimmunoprecipitated with topo IIα by using anti-topo IIα rabbit sera, but not using rabbit IgG. P, precipitated proteins; S, nonprecipitated supernatant proteins. Representative blot from eight independent experiments. (B) Full-length APC immunoprecipitated with affinity-purified polyclonal anti-APC sera (left and middle). Endogenous topo IIα (top) coimmunoprecipitated with the endogenous full-length APC, whereas topo IIβ did not (bottom). Quantification of the band intensity from three independent experiments revealed 1.8% of the total topo IIα coprecipitated with full-length APC (right). Representative blots from seven independent experiments. (C) Colocalization of endogenous APC and topo IIα in HCT 116βw cells by using APC antibody (ab-7), polyclonal topo IIα antibody, and confocal microscopy. (a) Confocal image shows APC (green) and topo IIα (red) colocalized in the nucleus (yellow in merge). Bar, 5 μm. (b) Confocal images through the entire cell thickness were collected for APC (green) and topo IIα (red) and are shown as a projection of the 3-D Z-series images. (c) Overlapping pixels for the Z-series images in b are projected and shown in yellow. (d) Graph shows the average number of overlapping pixels calculated from six individual Z-series images; 1.9% of the topo IIα pixels overlap with APC, whereas 10% of the APC pixels overlap with topo IIα. (D) Measurements of FRET between APC-Alexa 488 and topo IIα-Alexa 568 were performed using the method of donor fluorescence sensitization after acceptor photobleaching in fixed samples of immunofluorescently labeled HCT116βw cells. Endogenous APC was labeled using either anti-APC ab-1 or anti-APC ab-7 followed by goat anti-mouse Alexa 488 secondary antibody. Endogenous topo IIα was labeled using anti-topo IIα antibody followed by goat anti-rabbit Alexa 568 secondary antibody. Energy transfer efficiencies (E) between immunolabeled Alexa 488-APC and Alexa 568-topo IIα were ~20.8% (gray bar, left, n = 10) within photobleached regions. This value is significantly positive (*p = 0.00021) compared with E measured without photobleaching (E = −0.9%, n = 10, white bar) or to energy transfer (E = −6.6%, n = 3, gray bar, right) between photobleached GFP (**p = 0.0000000056), which is abundantly expressed in the nucleus and immunolabeled Alexa 488-APC.

tently detected nearly 2% of the total topo IIα coprecipitated with APC (Figure 1B, right). In contrast, although topoisomerase IIβ is 75% identical to topo IIα, topo IIβ did not coprecipitate with APC (Figure 1B, left). This apparent binding preference for topo IIα over topo IIβ increases the likelihood that the APC-topo IIα interaction is specific.

The subcellular distribution of endogenous APC and topo IIα further implicated topo IIα as a binding partner of APC. Endogenous APC was found to colocalize with topo IIα within single confocal slices taken through the nucleus where both occur as overlapping puncta (Figure 1Ca). When the entire cell thickness was visualized by a series of confocal images captured in the z-plane, areas of overlap were apparent throughout the nuclei (Figure 1Cb). To show the areas of overlap from an entire cell thickness as a single image, overlapping signals in the 3-D data sets were projected onto a 2-D surface and are displayed in yellow (Figure 1Cc). The degree of overlap between the corresponding regions was calculated for each 2-D confocal section and is displayed as the average for the entire imaged volume. On average, 1.9% of the topo IIα signal coincided with APC, and 10% of the APC signal coincided with topo IIα (Figure 1Cd).

To further examine the association between APC and topo IIα, we analyzed FRET between the two immunolabeled proteins in fixed, permeabilized HCT116βw cells (Figure 1D). Given the nature of FRET, it is estimated that energy transfer would be detected only if two antibody-labeled proteins are <30 nm apart. Detection of an average energy transfer efficiency (E) of 20.8% between immunolabeled Alexa 488-APC and Alexa 568-topo IIα within photobleached regions of interest indicates that endogenous APC and topo IIα are in proximity and is consistent with a direct interaction in colon epithelial cells. This value is significantly more positive than measurements performed on cells in which photobleaching was omitted (E = −0.9%). Likewise, cells transiently expressing GFP showed no energy transfer between endogenous topo IIα and exogenous GFP (E = −6.6%), even though GFP was abundant in the nucleus (see, e.g., Figure 5A).

The 15-Amino Acid Repeat Region of APC Colocalizes with Topo IIα, Alters Nuclear Morphology, and Causes Cell Cycle Arrest in G2

APC is a 310-kDa protein with several distinct protein binding domains (Figure 2A). To identify potential topo IIα

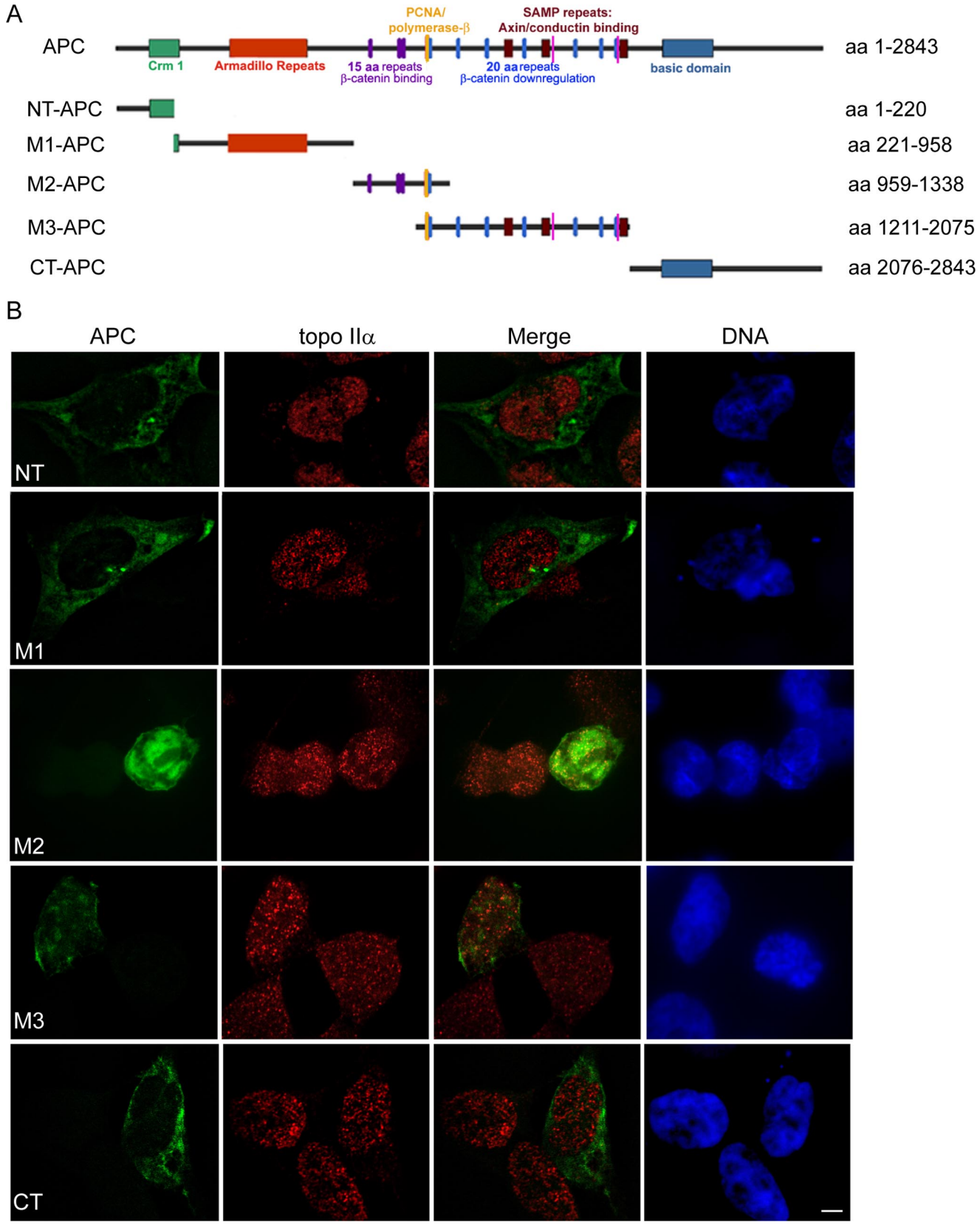

Figure 2. The 15-amino acid and 20-amino acid repeat regions of APC each colocalize with topo IIα and localize to the nucleus. (A) Schematic diagram of APC with domains implicated in nuclear function marked. Two NLSs are designated by thin pink lines in both full-length APC and M3-APC. Five APC fragments expressed as GFP fusions are shown. (B) Colocalization of the GFP-fused APC fragments with endogenous topo IIα in HCT116βw cells. Of the five APC fragments, both M2 and M3 displayed significant nuclear localization and partial colocalization with topo IIα. Bar, 5 μm.

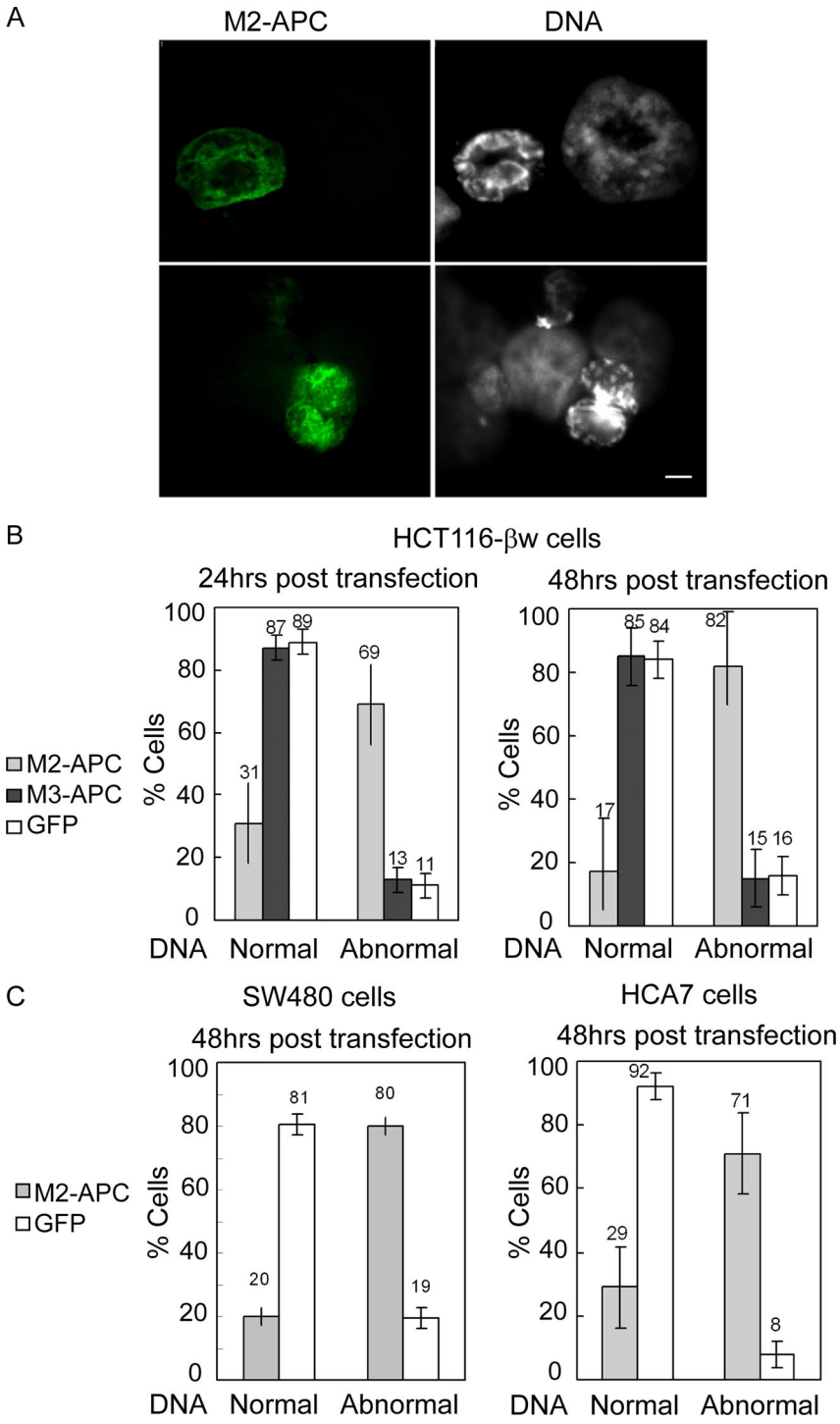

Figure 3. The 15-amino acid repeat region of APC protein alters nuclear morphology. (A) Confocal immunofluorescence microscopy revealed abnormal nuclei (condensed or fragmented) in M2-APC–expressing HCT116βw cells. Bar, 5 μm. (B) Nuclear phenotype of HCT116βw cells expressing GFP-M2-APC (light bar), GFP-M3-APC (dark bar), or GFP (white bar) at 24 and 48 h after transfection. More than 80% of the M2-APC–expressing cells displayed abnormal nuclear morphology by 48 h. (C) Nuclear phenotype of SW480 cells and HCA7 cells expressing GFP-M2-APC (light bar) or GFP (white bar) at 48 h after transfection. (B and C) Graphs represent analysis of 100 cells for each transfection in three independent experiments, with error bars indicating SD.

binding domains in APC, we expressed five GFP-fused APC fragments (Figure 2A) in HCT116βw cells and compared their localization with that of endogenous topo IIα (Figure 2B). As expected, GFP fused with either NT-APC, M1-APC, or CT-APC predominantly localized to the cytoplasm (Figure 2B). M3-APC (amino acids 1211–2075) contains all 20-amino acid repeats and two nuclear localization signals (NLSs) (Zhang *et al*., 2000) and appeared to be located in the nucleus when fused to GFP. GFP fused with M2-APC (amino acids 959-1338) showed the most prominent overlap with topo IIα in the nucleus. This region of APC contains all four 15-amino acid β-catenin binding repeats and one 20 amino acid repeat but no defined NLS.

Not only was GFP-M2-APC predominantly localized to the nucleus but also HCT116βw cells expressing this APC fragment displayed abnormal DNA morphology, with nuclei looking condensed or fragmented (Figure 3A). To quantify this phenotype, GFP-positive cells were scored at 24, 48, and 72 h after transfection (Figure 3B and Supplemental Table 1). GFP-M2-APC expression resulted in a dramatic alteration in the DNA morphology, with 82% of the cells displaying abnormal nuclei by 48 h after transfection. In

contrast, expression of GFP-M3-APC or GFP alone had little effect on DNA morphology. Because the abnormal nuclear morphology was not prevalent in M3-APC– or GFP-expressing cells, but rather was limited to cells expressing M2-APC, this phenotype is not merely the cellular response to overexpression of a nuclear protein. Moreover, abnormal nuclei were also observed in SW480, HCA7 (Figure 3C and Supplemental Table 1) and parental HCT116 cells (data not shown) expressing GFP-M2-APC. Therefore, the abnormal nuclear morphology is not restricted to the HCT116βw cell line and is not dependent on full-length endogenous APC.

The abnormal nuclear morphology resulting from M2-APC expression resembled that seen in apoptotic cells. To determine whether overexpression of M2-APC triggered apoptosis, we examined cells for various apoptotic markers such as activated caspase-3 and annexin V, but we found no evidence of apoptosis (data not shown). Furthermore, when the cell cycle distribution of propidium iodide-stained cells was analyzed using FACS analysis, the GFP-M2-APC–expressing cells had no detectable sub-G0 cell population indicative of apoptotic cells (Figure 4A). Overall, the cell cycle distribution of nontransfected cells was only slightly different from that of GFP-expressing cells. In contrast, the GFP-M2-APC–expressing cells showed a reproducible 2.5-fold increase in the G2/M phase and an accompanying reduction in the S phase compared with control cells (Figure 4B).

To determine whether this expanded G2/M population reflected an arrest in the G2 or M phase of the cell cycle, mitotic indices and phospho-histone H3 expression were both evaluated at 24, 48, and 72 h after transfection (Figure 4, C and D). None of the M2-APC–expressing cells were mitotic at any time, whereas control cells that were not transfected or expressed GFP alone showed typical mitotic indices at all times examined. These data suggest that the expression of M2-APC results in G2 cell cycle arrest.

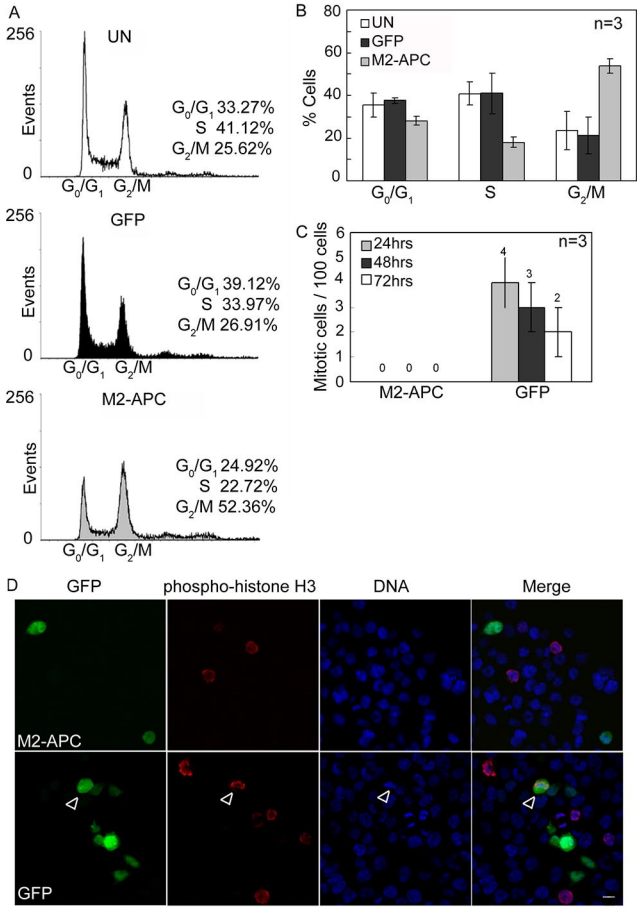

Figure 4. Expression of the 15-amino acid repeat region of APC results in G2 accumulation. (A) Histograms showing representative FACS displays of cell cycle distribution assessed by propidium iodide staining. UN, untransfected cells. For both GFP- and GFP-M2-APC–expressing cells, only GFP-positive cells are displayed. (B) FACS data from three independent experiments. The fraction of cells in G2/M doubled, and the S phase decreased by half for cells expressing GFP-M2-APC compared with the untransfected control cells or cells expressing only GFP. Values for G0/G1, S, and G2/M, respectively, are 35.6 ± 2.1, 40.9 ± 2.4, and 23.5 ± 3.3% (for untransfected); 37.7 ± 1.3, 41.0 ± 9.6, and 21.3 ± 8.5% (for GFP); and 28.0 ± 5.6, 18.1 ± 5.6, and 53.9 ± 8.9% (for M2-APC). For each transfection, 15,000 GFP-positive cells were analyzed. (C) Mitotic events assessed after DAPI staining. One hundred randomly chosen M2-APC– or GFP-expressing cells were analyzed from three independent experiments at 24, 48, and 72 h after transfection. None of the M2-APC–expressing cells appeared to be mitotic. A small number of the GFP-expressing cells were mitotic. (D) Representative immunofluorescence confocal microscopy of mitotic marker phospho-histone H3 from three independent experiments. No M2-APC–expressing cells were positive for phospho-histone H3, whereas a few GFP-expressing cells were positive. Arrowhead indicates a cell that is positive for both GFP and phospho-histone H3. Bar, 10 μm.

The Abnormal Nuclear Morphology after Expression of the 15-Amino Acid Repeat of APC Is Not Due to Altered β-Catenin

M2-APC comprises all four of the 15-amino acid β-catenin binding repeats and one of the 20-amino acid repeats involved in β-catenin down-regulation (Figure 2A). Activated Wnt signaling resulting from stabilized β-catenin was recently reported to contribute to chromosome instability (Aoki *et al*., 2007) and lead to G2 arrest (Olmeda *et al*., 2003). Thus, we predicted that the abnormal nuclear morphology seen in cells expressing M2-APC was dependent on M2-APC association with and stabilization of nuclear β-catenin. We found β-catenin expression and localization identical in HCT116βw cells expressing M2-APC, GFP, or nontransfected (Figure 5A). Furthermore, immunoblots from total lysates demonstrated comparable levels of β-catenin in M2-APC– and GFP-expressing cells (Figure 5D). Moreover, <1% of the total β-catenin coprecipitated with GFP-M2-APC (Figure 5B). In contrast, >10% of the total β-catenin was precipitated along with endogenous full-length APC in parallel experiments under the same experimental conditions (Figure 5C). Finally, β-catenin activity measured in M2-APC–expressing cells was comparable with that in GFP-expressing cells (Figure 5E). Thus, it seems unlikely that the abnormal nuclear morphology and the G2 cell cycle arrest observed in M2-APC–expressing cells result from β-catenin sequestration by M2-APC.

The 15-Amino Acid Repeat Region of APC Interacts with Topo IIα

Our original identification of APC in complex with topo IIα, an essential regulator of the G2/M transition prompted us to examine whether M2-APC could interact with topo IIα and possibly mediate the G2 arrest through this interaction. HCT116βw cells transiently expressing M2-APC had increased levels of total topo IIα (Figure 6A) and the topo IIα coprecipitated with GFP-M2-APC (Figure 6B). In contrast,

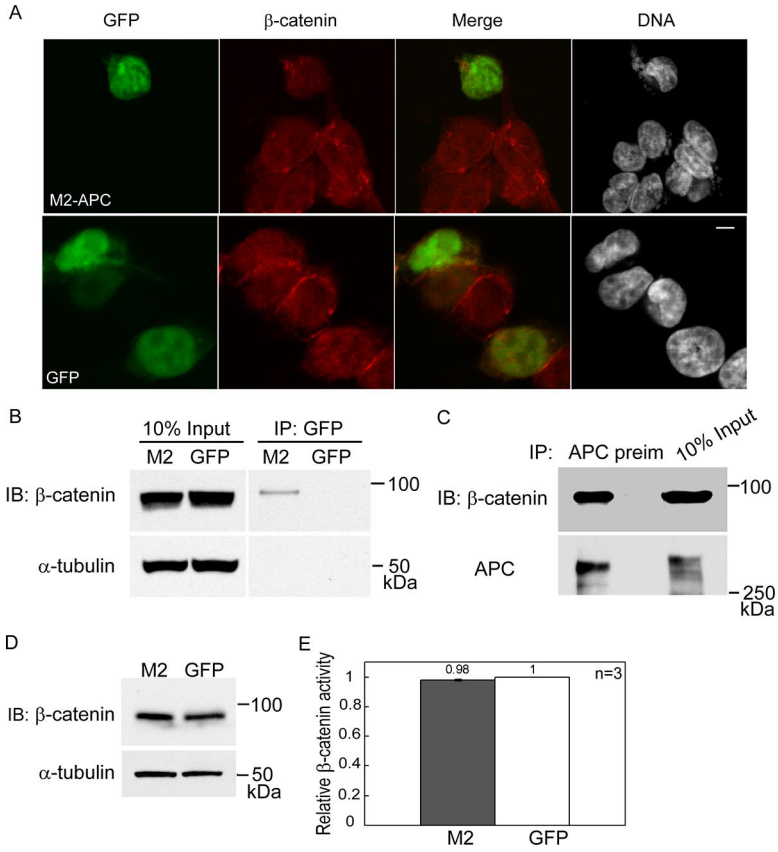

Figure 5. Expression of the 15-amino acid repeat region of APC does not alter β-catenin expression or localization. (A) Confocal immunofluorescence microscopy reveals similar β-catenin localization in M2-APC– and GFP-expressing HCT116βw cells. Note that the nucleus (right) is abnormal in the M2-APC–expressing cell. Bar, 5 μm. (B) Less than 1% of the total β-catenin coimmunoprecipitated with GFP-M2-APC by using a GFP antibody (M2), and none coimmunoprecipitated with GFP alone (GFP). Ten percent input is 25 μg of total protein. Transfection efficiency was ~50%. (C) Nearly 10% of the total β-catenin coimmunoprecipitated with endogenous APC. Ten percent input is 30 μg of total protein. Representative blots from five independent experiments. (D) Western blot reveals comparable levels of total β-catenin in M2-APC- (M2) and GFP-expressing (GFP) cells. Equivalent amounts of total protein from whole cell lysates were loaded. (B and D) Representative blots from three independent experiments. (E) Cells were cotransfected with GFP-M2-APC or GFP, SuperTOP-flash or FOP-flash reporters, and pRL-TK *Renilla* luciferase plasmid. Luciferase activities were determined 24 h after transfection and normalized against both pRL-TK *Renilla* activity and FOP-flash reporter activity. Values are mean ± SD for triplicate samples from a representative experiment.

no topo IIα precipitated with the GFP in cells expressing GFP alone. Because M2-APC and topo IIα interact, it is possible that M2-APC can influence the activity of topo IIα. To test this directly, in vitro DNA relaxation and decatenation assays were performed using purified recombinant proteins topo IIα and M2-APC. Purified M2-APC stimulated topo IIα activity in both DNA relaxation (Figure 6C) and decatenation assays (data not shown). This enhancement was apparent when purified M2-APC was provided at equal molar concentration to the topo IIα and was further pronounced with 4 times more M2-APC in the reaction (Figure 6C). In the absence of topo IIα, purified M2-APC did not relax the DNA (Figure 6C) or bind to the DNA slowing its migration (data not shown). Using a higher concentration of recombinant topo IIα, M2-APC still enhanced topo IIα activity (Figure 6D). In contrast, bovine serum albumin (BSA)

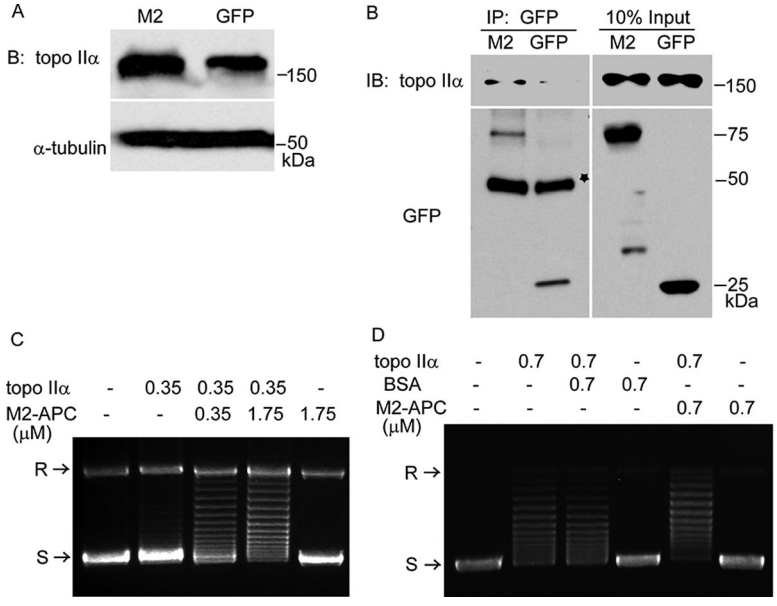

Figure 6. The 15-amino acid repeat region of APC associates with topo IIα and enhances topo IIα activity. (A) Increased expression of topo IIα in M2-APC–expressing cells compared with GFP-expressing cells. Equivalent total protein loaded in each lane. (B) Topo IIα coimmunoprecipitates with M2-APC, but not with GFP. Ten percent input is 25 μg of total protein. The star marks migration of antibody heavy chain. (A and B) Representative blots from five independent experiments. (C and D) Representative topo IIα DNA relaxation assays from five independent experiments. R, relaxed plasmid DNA; S, supercoiled plasmid. (C) Purified recombinant human topo IIα (0.35 μM) slightly relaxed supercoiled plasmid DNA (lane 2). Addition of purified recombinant M2-APC (0.35 or 1.75 μM) to the reaction resulted in progressively enhanced topo IIα plasmid relaxation activity (lanes 3 and 4). M2-APC did not have plasmid relaxation activity in the absence of topo IIα (lane 5). (D) Using a higher concentration of topo IIα (0.7 μM), the addition of BSA (0.7 μM) did not enhance the plasmid relaxation activity, but rather slightly inhibited it (compare lanes 2 and 3). M2-APC (0.7 μM) enhanced the plasmid relaxation activity (lane 5).

protein at an equal molar ratio slightly inhibited topo IIα activity (Figure 6D). These in vitro assays provide additional support for a functional interaction between APC and topo IIα. Together, our data implicate topo IIα as a mediator of abnormal DNA morphology and G2 arrest associated with exogenous M2-APC expression.

DISCUSSION

In this study, we identify a novel interaction between the tumor suppressor protein APC and topo IIα. This interaction was demonstrated by colocalization, reciprocal coimmunoprecipitation, FRET, and functional assays. Topo IIα interacts with the 15-amino acid repeat region of APC (M2-APC, amino acids 959-1338). When overexpressed in colon cancer cell lines, M2-APC located predominantly to the nucleus. Cells expressing M2-APC displayed abnormal nuclear morphology and were inhibited in the G2 phase of the cell cycle. Although M2-APC could bind β-catenin, we found no evidence supporting a role for β-catenin in the observed phenotypes. Our data suggest a novel role for nuclear APC in the regulation of cell cycle progression, potentially through an interaction between topo IIα and the 15-amino acid repeat region of APC.

The GFP–M2-APC protein was not expected to locate predominantly to the nucleus. Although endogenous full-length APC exists in both cytoplasm and nucleus (Neufeld and White, 1997; Anderson *et al*., 2002), the classic NLSs that are thought to facilitate nuclear localization of APC (Zhang *et al*., 2000) are not present in the M2-APC fragment. The M2-APC region is retained in most truncated forms of APC associated with colorectal cancer and these truncated APC proteins are capable of nucleocytoplasmic shuttling (Fagman *et al*., 2003). However, the nuclear import ability of these truncated APC proteins has been attributed to the armadillo repeat region (amino acids 334–625), not the 15-amino acid repeat region (Galea *et al*., 2001). With an estimated molecular weight of ~70 kDa, GFP-M2-APC is too large to enter the nucleus by diffusion, which has a size limitation of 30–50 kDa (Schulz and Peters, 1987; Mattaj and Englmeier, 1998; Moroianu, 1999). Therefore, M2-APC likely contains a nonstandard NLS or is carried into the nucleus by a nuclear binding partner. Because here we show that M2-APC binds to the abundant nuclear protein topo IIα, it is possible that nuclear entry of M2-APC is facilitated in part by topo IIα. APC has also been reported to bind PCNA through the M2 region (Narayan *et al*., 2005), and we have confirmed that PCNA coimmunoprecipitates with M2-APC (data not shown). We reason that other nuclear proteins, such as PCNA, might contribute to the nuclear entry of M2-APC as well.

As an abundant nuclear protein, topo IIα is involved in several processes throughout the cell cycle, including transcription, DNA replication, chromatin recombination and organization, and regulation of the G2 decatenation checkpoint (Wang, 1996; Nitiss, 1998; Fortune and Osheroff, 2000; Champoux, 2001; Wang, 2002; McClendon and Osheroff, 2007). It is possible that the topo IIα we consistently found associated with endogenous APC and with the M2-APC fragment (Figures 1B and 6B) corresponds to a specific pool of topo IIα involved in regulation of the G2/M transition. Other pools of topo IIα might be positioned near replicating heterochromatin during S phase (Agostinho *et al*., 2004), tightly associated with DNA to aid chromosome assembly at the G2/M transition (Earnshaw and Heck, 1985; Gasser *et al*., 1986; Swedlow and Hirano, 2003), responsible for transcription regulation at G1/S (Huang *et al*., 2007), or involved in chromosome segregation at the exit of mitosis (Hirano and Mitchison, 1993; Downes *et al*., 1994; Grue *et al*., 1998). One explanation for the rather modest amount of topo IIα that coprecipitated with endogenous APC is that the interaction between APC and topo IIα is transient, only occurring at a specific point of the cell cycle.

APC is not the first tumor suppressor protein to interact with topo IIα. BRCA1 (Yamane *et al*., 2003; Lou *et al*., 2005), RB (Bhat *et al*., 1999), and p53 (Cowell *et al*., 2000) each bind to topo IIα and thereby effect topo IIα functions. A recent report also links topo IIα to the oncoprotein β-catenin and its transcription cofactor TCF (Huang *et al*., 2007). Overexpression of topo IIα led to enhanced β-catenin/TCF transcription activity, whereas expression of a constitutively active β-catenin led to increased topo IIα activity measured in a whole cell lysate. We predict that β-catenin/TCF associates with a topo IIα pool that is involved in transcription regulation at G1/S. It is possible that this interaction is indirect and mediated by APC. APC has been found in association with the enhancer region of genes regulated by β-catenin/TCF (Sierra *et al*., 2006). In contrast, we suspect that the APC/topo IIα interaction we described here is direct. Purified recombinant human M2-APC enhanced the plasmid relaxation activity of purified topo IIα in our in vitro assays which lacked other potential linker proteins (Figure 6, C and D). Moreover, M2-APC does not seem to bind directly to DNA as determined by gel shift assays (data not shown). We propose that the pool of topo IIα that interacts with APC to impact G2 cell cycle transition is separate from the pool involved in β-catenin mediated transcription.

We report that the topo IIα protein level was higher in cells expressing GFP-M2-APC than in GFP-expressing cells (Figure 6A). This observation is consistent with previous reports that topo IIα levels peak in G2 (Heck *et al*., 1988). We also report that purified M2-APC enhances topo IIα activity in an in vitro relaxation assay (Figure 6, C and D). Cell cycle progression from G2 to M is likely dependent on the maintenance of topo IIα activity at a precise level. Indeed, Epstein-Barr virus kinase BGLF4 both stimulates topo IIα activity and induces premature chromosome condensation similar to the abnormal DNA morphology we report with M2-APC expression (Lee *et al*., 2007). Furthermore, protein kinase Cδ regulates topo IIα activity specifically during S phase with aberrant activation of topo IIα by protein kinase Cδ leading to apoptosis (Yoshida *et al*., 2006). At the simplest level, we propose that endogenous APC regulates topo IIα activity and thereby facilitates G2-M cell cycle progression.

Topo IIα activity is essential for the chromatin decatenation required before mitosis (Downes *et al*., 1994). APC locates near centrosomes during early and late stages of mitosis and has also been implicated in maintenance of chromatin structure (Olmeda *et al*., 2003; Huang *et al*., 2007). Therefore, we cannot exclude the possibility that both APC and topo IIα provide multiple functions throughout the G2/M transition. We propose that a functional interaction between APC and topo IIα results in regulation of topo IIα activity. Without this regulation, cell cycle progression would be affected. Given that truncated APC found in most colorectal cancers includes the M2-APC region, it is possible that topo IIα regulation is maintained in these cancers. In this scenario, retention of the topo IIα regulatory domain in truncated APC might be essential for cell viability. Alternatively, truncated APC proteins associated with cancer might behave more like the M2-APC fragment and be unable to effectively regulate topo IIα activity. The resulting stimulation of DNA cleavage by topo IIα would be predicted to induce chromosome instability, a hallmark of cancer.

Together, we propose a novel function for the tumor suppressor APC in regulation of the G2-M cell cycle transition, potentially through interaction with topo IIα. Future investigation will be needed to determine the precise underlying mechanism by which M2-APC promotes G2 cell cycle arrest. Such studies will potentially reveal a novel activity of APC in tumor suppression. This expanded role of the tumor suppressor APC has obvious implications in explaining the deregulation of topo IIα in colon cancer tissue (Murphy *et al*., 2001) and for the use of topo IIα inhibitors as chemotherapeutic agents to treat colorectal cancer.

ACKNOWLEDGMENTS

We thank Kozo Kaibuchi (Nagoya University, Japan) for providing expression constructs for APC fragments fused to GFP, Bert Vogelstein (The Johns Hopkins University) for providing the HCT 116βw (mut ko, β-cat w/-) cell line, Susan Kirkland (Imperial College London) for providing the HCA-7 cell line, Joe Holden (University of Utah) for providing the anti-topo IIα sera, Robert Coffey (Vanderbilt University) for providing reagents and reviewing the manuscript, and Jo Ann Byl (Vanderbilt University) for providing technical support with the topoisomerase activity assays. This work was funded by National Institutes of Health grants R01 CA-10922 (to Y. W. and K.L.N.) and GM-33944 (to N. O.) and by Higuchi Biosciences Center J.R. & Inez Jay Award (to Y. W., Y. A., and K.L.N.).

REFERENCES

Agostinho, M., Rino, J., Braga, J., Ferreira, F., Steffensen, S., and Ferreira, J. (2004). Human topoisomerase IIalpha: targeting to subchromosomal sites of activity during interphase and mitosis. Mol. Biol. Cell *15*, 2388–2400.

Anderson, C. B., Neufeld, K. L., and White, R. L. (2002). Subcellular distribution of Wnt pathway proteins in normal and neoplastic colon. Proc. Natl. Acad. Sci. USA *99*, 8683–8688.

Aoki, K. *et al*. (2007). Chromosomal instability by beta-catenin/TCF transcription in APC or beta-catenin mutant cells. Oncogene *26*, 3511–3520.

Azuma, Y., Arnaoutov, A., and Dasso, M. (2003). SUMO-2/3 regulates topoisomerase II in mitosis. J. Cell Biol. *163*, 477–487.

Bhat, U. G., Raychaudhuri, P., and Beck, W. T. (1999). Functional interaction between human topoisomerase IIalpha and retinoblastoma protein. Proc. Natl. Acad. Sci. USA *96*, 7859–7864.

Bhattacharjee, R. N., Hamada, F., Toyoshima, K., and Akiyama, T. (1996). The tumor suppressor gene product APC is hyperphosphorylated during the M phase. Biochem. Biophys. Res. Commun. *220*, 192–195.

Bolte, S., and Cordelieres, F. P. (2006). A guided tour into subcellular colocalization analysis in light microscopy. J. Microsc. *224*, 213–232.

Champoux, J. J. (2001). DNA topoisomerases: structure, function, and mechanism. Annu. Rev. Biochem. *70*, 369–413.

Chan, T. A., Wang, Z., Dang, L. H., Vogelstein, B., and Kinzler, K. W. (2002). Targeted inactivation of CTNNB1 reveals unexpected effects of beta-catenin mutation. Proc. Natl. Acad. Sci. USA *99*, 8265–8270.

Cowell, I. G., Okorokov, A. L., Cutts, S. A., Padget, K., Bell, M., Milner, J., and Austin, C. A. (2000). Human topoisomerase IIalpha and IIbeta interact with the C-terminal region of p53. Exp. Cell Res. *255*, 86–94.

Downes, C. S., Clarke, D. J., Mullinger, A. M., Gimenez-Abian, J. F., Creighton, A. M., and Johnson, R. T. (1994). A topoisomerase II-dependent G2 cycle checkpoint in mammalian cells. Nature *372*, 467–470.

Earnshaw, W. C., and Heck, M. M. (1985). Localization of topoisomerase II in mitotic chromosomes. J. Cell Biol. *100*, 1716–1725.

Fagman, H., Larsson, F., Arvidsson, Y., Meuller, J., Nordling, M., Martinsson, T., Helmbrecht, K., Brabant, G., and Nilsson, M. (2003). Nuclear accumulation of full-length and truncated adenomatous polyposis coli protein in tumor cells depends on proliferation. Oncogene *22*, 6013–6022.

Fodde, R. *et al*. (2001). Mutations in the APC tumour suppressor gene cause chromosomal instability. Nat. Cell Biol. *3*, 433–438.

Fortune, J. M., and Osheroff, N. (2000). Topoisomerase II as a target for anticancer drugs: when enzymes stop being nice. Prog. Nucleic Acid Res. Mol. Biol. *64*, 221–253.

Fortune, J. M., and Osheroff, N. (2001). Topoisomerase II-catalyzed relaxation and catenation of plasmid DNA. Methods Mol. Biol. *95*, 275–281.

Galea, M. A., Eleftheriou, A., and Henderson, B. R. (2001). ARM domain-dependent nuclear import of adenomatous polyposis coli protein is stimulated by the B56 alpha subunit of protein phosphatase 2A. J. Biol. Chem. *276*, 45833–45839.

Gasser, S. M., Laroche, T., Falquet, J., Boy de la Tour, E., and Laemmli, U. K. (1986). Metaphase chromosome structure. Involvement of topoisomerase II. J. Mol. Biol. *188*, 613–629.

Grue, P., Grasser, A., Sehested, M., Jensen, P. B., Uhse, A., Straub, T., Ness, W., and Boege, F. (1998). Essential mitotic functions of DNA topoisomerase IIalpha are not adopted by topoisomerase IIbeta in human H69 cells. J. Biol. Chem. *273*, 33660–33666.

Heck, M. M., Hittelman, W. N., and Earnshaw, W. C. (1988). Differential expression of DNA topoisomerases I and II during the eukaryotic cell cycle. Proc. Natl. Acad. Sci. USA *85*, 1086–1090.

Heinen, C. D., Goss, K. H., Cornelius, J. R., Babcock, G. F., Knudsen, E. S., Kowalik, T., and Groden, J. (2002). The APC tumor suppressor controls entry into S-phase through its ability to regulate the cyclin D/RB pathway. Gastroenterology *123*, 751–763.

Hirano, T., and Mitchison, T. J. (1993). Topoisomerase II does not play a scaffolding role in the organization of mitotic chromosomes assembled in *Xenopus* egg extracts. J. Cell Biol. *120*, 601–612.

Huang, L., Shitashige, M., Satow, R., Honda, K., Ono, M., Yun, J., Tomida, A., Tsuruo, T., Hirohashi, S., and Yamada, T. (2007). Functional interaction of DNA topoisomerase IIalpha with the beta-catenin and T-cell factor-4 complex. Gastroenterology *133*, 1569–1578.

Ishidate, T., Matsumine, A., Toyoshima, K., and Akiyama, T. (2000). The APC-hDLG complex negatively regulates cell cycle progression from the G0/G1 to S phase. Oncogene *19*, 365–372.

Jaiswal, A. S., and Narayan, S. (2004). Zinc stabilizes adenomatous polyposis coli (APC) protein levels and induces cell cycle arrest in colon cancer cells. J. Cell Biochem. *93*, 345–357.

Kaplan, K. B., Burds, A. A., Swedlow, J. R., Bekir, S. S., Sorger, P. K., and Nathke, I. S. (2001). A role for the Adenomatous Polyposis Coli protein in chromosome segregation. Nat. Cell Biol. *3*, 429–432.

Kenworthy, A. K., and Edidin, M. (1998). Distribution of a glycosylphosphatidylinositol-anchored protein at the apical surface of MDCK cells examined at a resolution of $<$100 A using imaging fluorescence resonance energy transfer. J. Cell Biol. *142*, 69–84.

Kingma, P. S., Greider, C. A., and Osheroff, N. (1997). Spontaneous DNA lesions poison human topoisomerase IIalpha and stimulate cleavage proximal to leukemic 11q23 chromosomal breakpoints. Biochemistry *36*, 5934–5939.

Kinzler, K. W., and Vogelstein, B. (1996). Lessons from hereditary colorectal cancer. Cell *87*, 159–170.

Lamm, G. M., Steinlein, P., Cotten, M., and Christofori, G. (1997). A rapid, quantitative and inexpensive method for detecting apoptosis by flow cytometry in transiently transfected cells. Nucleic Acids Res. *25*, 4855–4857.

Lazaris, A. C., Kavantzas, N. G., Zorzos, H. S., Tsavaris, N. V., and Davaris, P. S. (2002). Markers of drug resistance in relapsing colon cancer. J. Cancer Res. Clin. Oncol. *128*, 114–118.

Lee, C. P., Chen, J. Y., Wang, J. T., Kimura, K., Takemoto, A., Lu, C. C., and Chen, M. R. (2007). Epstein-Barr virus BGLF4 kinase induces premature chromosome condensation through activation of condensin and topoisomerase II. J. Virol. *81*, 5166–5180.

Lou, Z., Minter-Dykhouse, K., and Chen, J. (2005). BRCA1 participates in DNA decatenation. Nat. Struct. Mol. Biol. *12*, 589–593.

Mattaj, I. W., and Englmeier, L. (1998). Nucleocytoplasmic transport: the soluble phase. Annu. Rev. Biochem. *67*, 265–306.

McClendon, A. K., and Osheroff, N. (2007). DNA topoisomerase II, genotoxicity, and cancer. Mutat. Res. *623*, 83–97.

Moroianu, J. (1999). Nuclear import and export: transport factors, mechanisms and regulation. Crit. Rev. Eukaryot. Gene Expr. *9*, 89–106.

Murphy, K. J., Nielson, K. R., and Albertine, K. H. (2001). Defining a molecularly normal colon. J. Histochem. Cytochem. *49*, 667–668.

Narayan, S., Jaiswal, A. S., and Balusu, R. (2005). Tumor suppressor APC blocks DNA polymerase beta-dependent strand displacement synthesis during long patch but not short patch base excision repair and increases sensitivity to methylmethane sulfonate. J. Biol. Chem. *280*, 6942–6949.

Neufeld, K. L., and White, R. L. (1997). Nuclear and cytoplasmic localizations of the adenomatous polyposis coli protein. Proc. Natl. Acad. Sci. USA *94*, 3034–3039.

Nitiss, J. L. (1998). Investigating the biological functions of DNA topoisomerases in eukaryotic cells. Biochim. Biophys. Acta *1400*, 63–81.

Olmeda, D., Castel, S., Vilaro, S., and Cano, A. (2003). beta-Catenin regulation during the cell cycle: implications in G2/M and apoptosis. Mol. Biol. Cell *14*, 2844–2860.

Schulz, B., and Peters, R. (1987). Nucleocytoplasmic protein traffic in single mammalian cells studied by fluorescence microphotolysis. Biochim. Biophys. Acta *930*, 419–431.

Sierra, J., Yoshida, T., Joazeiro, C. A., and Jones, K. A. (2006). The APC tumor suppressor counteracts beta-catenin activation and H3K4 methylation at Wnt target genes. Genes Dev. *20*, 586–600.

Swedlow, J. R., and Hirano, T. (2003). The making of the mitotic chromosome: modern insights into classical questions. Mol. Cell *11*, 557–569.

Wang, J. C. (1996). DNA topoisomerases. Annu. Rev. Biochem. *65*, 635–692.

Wang, J. C. (2002). Cellular roles of DNA topoisomerases: a molecular perspective. Nat. Rev. Mol. Cell Biol. *3*, 430–440.

Watanabe, T., Wang, S., Noritake, J., Sato, K., Fukata, M., Takefuji, M., Nakagawa, M., Izumi, N., Akiyama, T., and Kaibuchi, K. (2004). Interaction with IQGAP1 links APC to Rac1, Cdc42, and actin filaments during cell polarization and migration. Dev Cell *7*, 871–883.

Worland, S. T., and Wang, J. C. (1989). Inducible overexpression, purification, and active site mapping of DNA topoisomerase II from the yeast *Saccharomyces cerevisiae*. J. Biol. Chem. *264*, 4412–4416.

Yamane, K., Chen, J., and Kinsella, T. J. (2003). Both DNA topoisomerase II-binding protein 1 and BRCA1 regulate the G2-M cell cycle checkpoint. Cancer Res. *63*, 3049–3053.

Yoshida, K., Yamaguchi, T., Shinagawa, H., Taira, N., Nakayama, K. I., and Miki, Y. (2006). Protein kinase C delta activates topoisomerase IIalpha to induce apoptotic cell death in response to DNA damage. Mol. Cell Biol. *26*, 3414–3431.

Zhang, F., White, R. L., and Neufeld, K. L. (2000). Phosphorylation near nuclear localization signal regulates nuclear import of adenomatous polyposis coli protein. Proc. Natl. Acad. Sci. USA *97*, 12577–12582.